Ultraluminous X-ray sources in dusty early-type galaxies

N. D. Vagshette, P. K. Pawar, M. K. Patil*

Abstract We present properties of 34 ULX sources detected within D_{25} region of 15 dusty early-type galaxies. All these sources have X-ray luminosity greater than 10^{39} erg s^{-1}, implying that they are resulted due to the accretion of matter on to compact object with mass $\geq 10 M_{\odot}$. Spectra of X-ray photons extracted from individual ULX are well represented by an absorbed power law with photon indices lying between 0.81 to 2.64, with their spectral properties closely matching with the hard-state spectra of the Galactic black hole binaries. The combined XLF of all the 34 ULXs is consistent with that reported earlier for early-type galaxies and is adequately descrbed by a power-law with slope equal to -1.34$\pm$0.12. The X-ray color-color plot of ULXs exhibit significant difference of their spectral properties with X-ray colors lying in the range between (-0.5, -0.5) to (+1.0, +1.0). We have quantified mass of a accreting sources on the basis of measured values of X-ray luminosities of individual ULXs and found to lie in the range between 20 $M_{\odot} \lesssim \mathbf{M} \lesssim$ 100 $M_{\odot}$.

Keywords galaxies: elliptical and lenticular, X-rays: binaries – X-rays:galaxies – X-ray:ULXs

1 Introduction

Imaging observations conducted with *Einstein* observatory during 1978 - 1981 have revealed that many of the galaxies host off-nuclear X-ray point like sources with their luminosities exceeding those of sources typically observed in the Milky Way and nearest neighbors (Fabbiano 1989). *ROSAT* during 1990s has observed hundreds of nearby galaxies and have detected several of such sources (Colbert & Mushotzky (1999), Roberts & Warwick (2000), Colbert & Ptak (2002)), however, it failed to investigate demographics of these objects. All these sources exhibit very high X-ray luminosities, defined as *Ultra Luminous X-ray Sources* (ULXs), with X-ray luminosities between $\sim 2\times 10^{39}$-10^{42} erg s^{-1}, i.e. significantly larger than the Eddington limit for a spherically accreting 10 $M_{\odot}$ black hole binary. Since their discovery by *Einstein* (Fabbiano & Trinchieri 1987), due to unusual characteristics, ULXs became targets of intense study with the later generation X-ray missions including ROSAT (Roberts & Warwick (2000), Colbert & Ptak (2002)), ASCA Makishima et al. (2000), *XMM-Newton* Strohmayer & Mushotzky (2003), and *Chandra* Coleman Miller & Colbert (2004). Despite of the large amount of data on these objects, their unusual nature remained controversial for years together.

The most intriguing idea proposed for explaining the unusual luminosity of ULXs was due to the accretion of matter on to the intermediate mass (10^2 - 10^5 $M_{\odot}$) black hole (IMBHs) (Fabbiano (1989), Kaaret (2001)). Existence of such IMBHs might be of great relevance in the sense that they may bridge the gap between the already known stellar mass black holes and the super massive black hole AGNs. Surprisingly, observational evidences have supported this concept of IMBH and have confirmed that at least some of the most luminous ULXs ($>10^{40}$ erg s^{-1}) are due to the accreting mass $\sim$ 1000 $M_{\odot}$ black holes (Roberts & Colbert 2003).

Systematic study of these sources with the *Chandra* and *XMM-Newton* have confirmed a large number of ULXs in a heterogeneous sample of external galaxies and have provided an excellent opportunity for systematic investigation of ULXs and also to constrain their nature. Generally, ULXs are found to be associated with the star forming regions (Swartz et al. (2009), Gilfanov et al. (2004)), and therefore their reliable detection in early-type galaxies is of considerable importance for understanding their nature. The present paper discuss X-ray emission properties of 34 ULXs de-

N. D. Vagshette, P. K. Pawar, M. K. Patil

School of Physical Sciences, Swami Ramanand Teerth Marathwada University Nanded, 431 606, India
e-mail: patil@iucaa.ernet.in

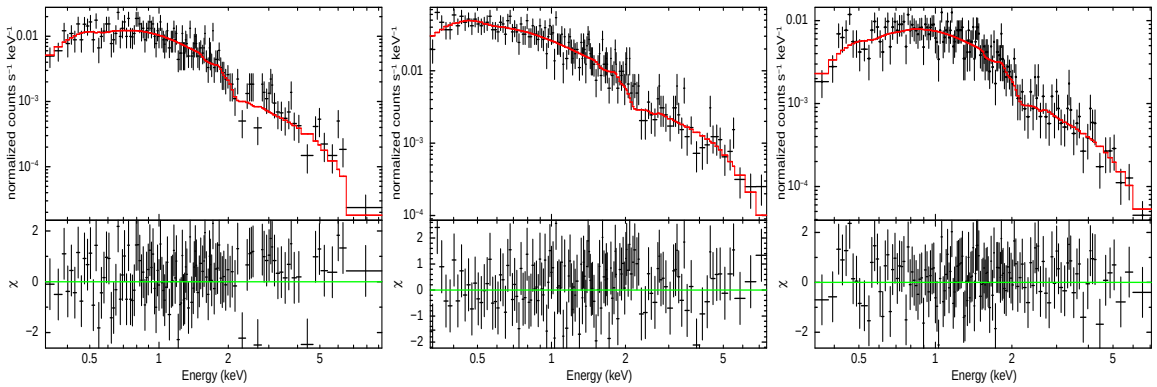

Fig. 1 Observed spectra of ULXs in NGC 4125 (left; src 16), NGC 4374 (middle; src 17) and NGC 5813 (right; src 31) and the best fit model consisting of PL modified by Galactic absorption.

tected within D_{25} region of 15 dusty early-type galaxies selected from different environments. All these X-ray sources exhibit their X-ray luminosity $> 10^{39}$ erg s^{-1}. This paper is arranged as follows: In Section 2 we outline the criteria for sample selection and data reduction. Results derived from this analysis are presented in Section 3, finally, we discuss the important results for the nature of ULXs in section 4. All the distance dependent estimates adopt H_0 = 70 km s^{-1} Mpc^{-1}.

2 Observation and data preparation

With an objective to investigate the X-ray emission properties of ULXs in a sample of early-type galaxies, we have selected a heterogeneous sample of 15 nearby dusty early-type galaxies from different environments i.e., isolated regions, groups and clusters. Here, we considered nearby objects with radial velocity $\leq$ 5000 km/s that had been observed for a total of at least 20 ks by the *Chandra* telescope. The global properties of sample galaxies and details of the *Chandra* observations are given in Table 1. Most of the sample galaxies were observed with the ACIS-S detector, except NGC 1395, where ACIS-I was employed. To achieve accuracy in the estimate of luminosity of each sources, literature survey was carried out for their reliable distance estimate.

The *Chandra* ACIS data were uniformly processed using the CIAO v4.2 and the latest calibrations files provided by the *Chandra* X-ray data Center (CALDB version 4.3.1). The periods during which count rate exceeded a certain threshold value (3σ) were identified as the "flare" periods and the data sets on the target galaxies were filtered out for these periods using the task *lc_sigma_clip* within CIAO v4.2. This resulted in to the good time intervals (GTI) of the X-ray events for each of the target galaxy and are listed in column 11 of Table 1. These light curve filtered event files were then used to detect the ULXs, spectral energy distribution of photons and for quantifying X-ray flux as well as luminosity of each of the source.

The source detection algorithm *wavdetect* available within CIAO was used to identify discrete high count rate X-ray point sources within D_{25} region of the full-band (0.3-10.0 keV) *Chandra* images on target galaxies (Pandge et al. (2012), Vagshette et al. (2012a)). Each of the elliptical area detected by the *wavdetect* algorithm (4σ of the PSF) was visually inspected and, if required, was modified accordingly. We extracted the spectra of those sources having counts grater than 50. The extraction regions are defined by *wavdetect* technique.To minimize the effect of spatial variation of diffuse emission due to CCD response, we extracted background counts from the annular region surrounding to individual source. Any source encompassed by the background region were excluded form the present study. Spectra for source and background region were generated in PI (pulse invariant) format. For each spectrum we created corresponding rmf (response matrices) and arf (ancillary response matrices) using *mkrmf* and *mkarf* tools. Spectral analysis of individual source was performed independently using the XSPEC (version 12.6.0) spectral fitting package and were grouped appropriately to ensure applicability of the χ^2 statistics.

3 Results

3.1 Spectral analysis

Spectra of all the ULX sources in 0.3-10.0 keV band were fitted with an absorbed power-law (PL) model and have provided the simplest phenomenological description for the acquired spectra. The absorption were fixed at Galactic values (Dickey & Lockman 1990). Using this model statistically acceptable ($\sim$ 90% confidence) fits were obtained for most of the sources. The best-fit parameters obtained for spectrum of an individual source with luminosity $> 10^{39}$ erg

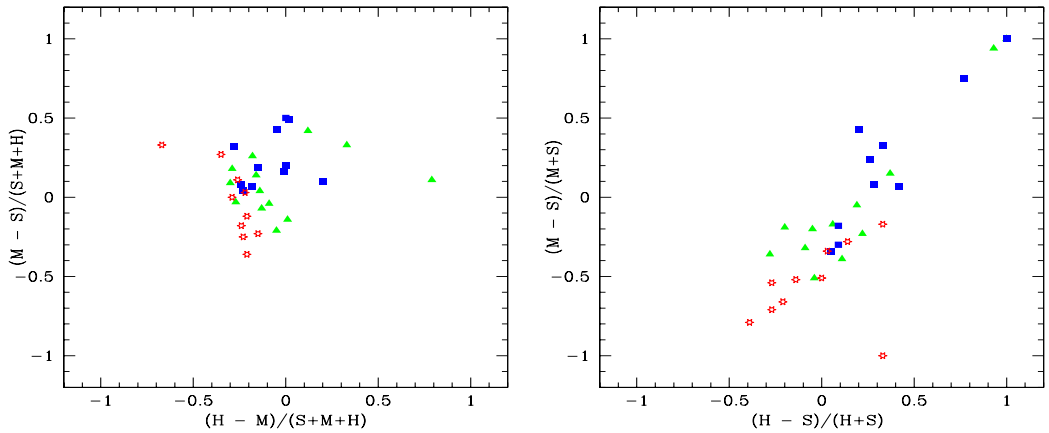

Fig. 2 Hardness ratio of the ULX sources; The open stars (red color) indicate the sources having photon index $\Gamma > 2$, green color triangles represent those with $1.5 < \Gamma < 2$ and blue color squares shows that $\Gamma < 1.5$

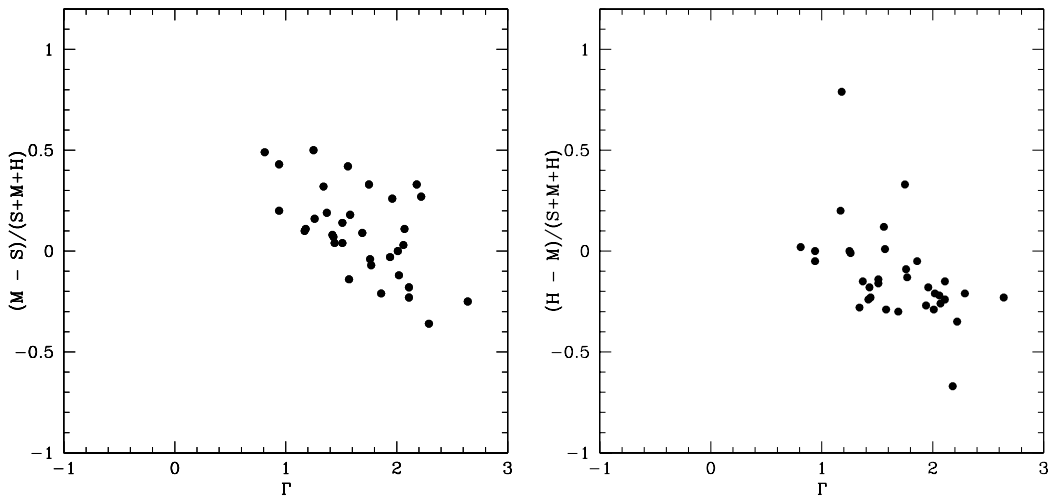

Fig. 3 The X-ray soft colors (left panel) & hard color (right panel) plotted against the photon index value of corresponding ULXs

s^{-1} along with their associated errors are presented in Table 2. All the errors are at the 90% confidence level. The detected ULX sources in sample galaxies are found to have their luminosities in the range between $1.03 \pm 0.25 \times 10^{39}$ erg s^{-1} to $7.33 \pm 0.39 \times 10^{39}$ erg s^{-1} and the photon index measured by an absorbed power-law model are found to range from 0.81 to 2.64. Fig. 1 shows the three sample spectra of ULXs with best fitted absorbed power-law (PL) model. Source No. 7 in Table 2 detected in NGC 1404 was initially fitted with single component, an absorbed power-law (PL) model, however the fit was not acceptable due their local absorption. Therefore we added second absorption component, which resulted in to best fit value of N_H = 3.0±1.52 $\times$ 10^{22} cm^{-2} and photon index of 1.18±0.78. Thus the src. No. 7 appears to be heavily absorbed harder source, perhaps a background AGN candidate.

3.2 Hardness ratio and luminosity function

In addition to fitting models to the 0.3 - 10.0 keV spectra of the highest count rate sources, the background subtracted X-ray counts for all extracted ULX sources were binned into three broad bands, defined as S(0.3-1.0 keV), M(1.0-2.0 keV) and H(2.0-10.0 keV). From this X-ray colors; soft color SC=(M-S)/T and hard color HC=(H-M)/T, where T = S+M+H, were constructed for individual source following the procedure described in Prestwich et al. (2001) and Vagshette et al. (2012b). The resultant X-ray colors of ULXs are given in column 9 & 10 of Table 2 and were also used to construct the X-ray color-color diagram for ULXs (Fig. 2, left panel).

The another method for deriving the color-color diagram has been used extensively in past studies using X-ray color definitions H21=(M-S)/(M+S) and H31=(H-S)/(H+S)

Table 1 Global parameters of the program galaxies

Sr. No.	Obj.	RA (J2000)	DEC (J2000)	Morph.	V_r (km/s)	z	Mag (M_B)	Obs-ID (arcmin)	Exp. (ks)	GTI (ks)	Environ
(1)	(2)	(3)	(4)	(5)	(6)	(7)	(8)	(9)	(10)	(11)	(12)
1	NGC 1395	03:38:29.8	-23:01:40	E2	1717	0.00573	10.97	799	28	22	BGG
2	NGC 1399	03:38:29.1	-35:27:03	E1	1425	0.00475	10.00	240	44	43	BCG
3	NGC 1404	03:38:51.9	-35:35:40	E1	1947	0.00649	10.95	2942	30	29	CG
4	NGC 1407	03:40:11.9	-18:34:49	E0	1779	0.00593	10.7	791	49	44.4	CG
5	NGC 2768	09:11:37.5	+60:02:14	S0	1373	0.00458	10.84	9528	65	64	FG
6	NGC 3379	10:47:49.6	+12:34:54	E1	911	0.00304	10.24	1587	32	30.9	FG
7	NGC 3923	11:13:17.1	-26:45:17	E7/S0	1434	0.00580	10.88	1563	22	15.60	BGG
8	NGC 4125	12:08:06.0	+65:10:27	E6	1356	0.00452	10.65	2071	65	62	BGG
9	NGC 4365	12:24:28.3	+07:19:04	E3	1243	0.00415	10.52	2015	41	40.4	CG
10	NGC 4374	12:25:03.7	+12:53:13	E1	1060	0.00354	10.09	803	29	27.8	CG
11	NGC 4473	12:29:48.9	+13:25:46	E5	2244	0.00749	11.16	4688	30	29.4	CG
12	NGC 4494	12:31:24.1	+25:46:31	E1-2	1344	0.00448	10.71	2079	25	22	GG
13	NGC 4649	12:43:40.0	+11:33:10	E2	1117	0.00373	9.81	8182	53	48.8	CG
14	NGC 4697	12:48:35.9	-05:48:03	E6	1241	0.00414	10.14	784	40	38	BGG
15	NGC 5813	15:01:11.2	+01:42:07	E1-2	1972	0.00658	11.45	9517	99	98.1	BGG

Note: col.2 - Target, col.3& 4 - right ascension & declination, respectively, col.5 - morphological type, col.6 - radial velocity, col.7 - redshift, col.8 - absolute magnitude in B band, col.9 - *Chandra* observation identification number Col. 10 - exposure time Col. 11 - good time interval (GTI) left after removal of periods of high background count rate Col. 12 - environment of galaxy; where GG: member of group galaxy; FG: Field galaxy; CG: member of cluster galaxy; BGG: brightest galaxy in group; BCG: brightest cluster galaxy

(Sarazin et al. (2000), Irwin et al. (2002)) and is shown in Fig. 2 (right panel)[1]. Six sources among 34 are found as harder sources having (H21, H31) $>$ (+0.5, +0.5) as four of them having (H21, H31)=(+1, +1).

Both the X-ray color-color diagram reveals a systematic pattern for ULXs, the open stars (red color) in these figure indicate the sources with photon index $\Gamma > 2$, filled triangles (green color) $1.5 < \Gamma < 2$, and squares (blue color) $\Gamma <$ 1.5. We have also tried to examine a correlation between the photon index of the ULXs with their X-ray color values and have noticed a marginal anti-correlation between the power law index and the soft and hard X-ray colors of the ULXs (Fig. 3).

With an objective to characterize the functional shape of the luminosity properties of ULXs we have derived the combined luminosity function of all the 34 sources and is shown in Fig. 4. The cumulative XLF of all the ULXs is adequately described by a simple power law function with a slope of -1.34$\pm$0.12.

4 Discussion

We have determined best-fit spectral parameters of the bright X-ray sources detected within D_{25} region of 15 nearby dusty early-type galaxies. The spectra of the ULXs are well fitted by absorbed power-law with photon index ranging from 0.81 to 2.64. Using the observed spectra and their corresponding best fit models are used to classify the sources as low/hard-state and high/soft-state. For this we assumed ULXs as isotropic emitters with spectra and luminosities is similar to those of the Galactic stellar mass X-ray binaries. This classification depends on (1) spectral shape (2) luminosity, and (3) position of X-ray sources within optical region (Winter et al. 2006). If ULXs are in low-state then spectra of the sources are well fitted by single power law, having luminosity ($L_X > 10^{38}$ erg s^{-1}) and that of all these sources i.e. within optical extent of the target galaxy (within D_{25} region). The high-sate ULXs are those sources having spectra characterized by an absorbed power-law plus MCD (or blackbody) model, luminosity and X-ray source within optical region.

The spectral fit parameters using single absorbed power law model (see Table 2) of 34 ULXs shows that these sources belongs to low (low/hard)-state class. Among the 34 sources, none of them was found as soft-excess component for high-state sources. Out of 34 ULXs, 21 sources follow the hard power law ($\Gamma < 1.8$) (like Zezas et al. (2002) in the Antennae, Soria et al. (2009) - NGC 1365 X-1 and X-2) while 13 sources exhibit soft $\Gamma > 1.8$. The lower L_X is associated with smaller Γ (hard power law) (see fig. 5), as in Galactic BHBs in low/hard state (Winter et al. 2006). Fig. 6 represent the distribution of power law photon index values of low-state ULXs, similar to the Galactic low-state objects with $\Gamma \approx 2.0$. As excess emission do not arise from the low-state object, therefore we expect the luminosity of

[1]All the sources found to lie along a diagonal line with their color values between (H21, H32)=(-0.36, -0.67) to (+1.0, +1.0)

Table 2 Spectral properties of ULXs

Src.No.	Obj (NGC)	RA (J2000)	DEC (J2000)	Γ	L_X (10^{39}erg s^{-1})	χ^2/dof	SC	HC	M_{BH} ($M_\odot$)
(1)	(2)	(3)	(4)	(5)	(6)	(7)	(8)	(9)	(10)
1	1395	03:38:30.517	-23:01:09.10	2.22±0.24	4.88±1.13	14.97/30=0.50	0.27	-0.35	98.0±22.60
2	1395	03:38:27.326	-23:02:40.35	2.29±0.48	2.12±0.57	10.91/13=0.84	-0.36	-0.21	42.40±11.40
3	1395	03:38:28.645	-23:02:29.04	1.17±0.77	1.43±0.54	10.08/10=1.01	0.1	0.2	28.60±10.80
4	1399	03:38:27.670	-35:26:48.79	2.18±0.65	2.55±1.05	3.64/4=0.91	0.33	-0.67	51.00±21.00
5	1399	03:38:21.920	-35:29:28.79	1.75±0.38	1.20±0.8	2.6/3=0.86	0.33	0.33	24.00±16.00
6	1404	03:38:52.002	-35:35:59.87	1.69±0.28	2.26±0.35	11.19/15=0.75	0.09	-0.3	45.20±7.00
7	1404	03:38:54.785	-35:35:01.08	1.18±0.78	7.33±1.31	3.70/7=0.53	0.11	0.79	147.0±33.60
8	1404	03:38:57.024	-35:35:32.81	0.94±0.48	1.54±0.47	6.05/6=1.01	0.2	0	30.80±9.40
9	1407	03:40:18.270	-18:36:01.76	1.58±0.32	2.59±0.35	12.63/19=0.66	0.18	-0.29	51.80±7.00
10	1407	03:40:14.515	-18:36:37.68	1.51±0.22	1.63±0.34	20.42/23=0.89	0.04	-0.14	32.60±6.80
11	1407	03:40:10.622	-18:35:43.07	1.37±0.20	1.12±0.28	10.15/13=0.79	0.19	-0.15	22.40±5.60
12	1407	03:40:12.525	-18:34:51.66	1.57±0.48	1.68±0.38	27.24/20=1.36	-0.14	0.01	33.60±7.60
13	2768	09:11:45.674	+60:01:36.56	0.81±0.42	1.11±0.22	18.41/18=1.02	0.49	0.02	22.20±4.40
14	3379	10:47:49.998	+12:34:56.70	1.94±0.10	2.43±0.15	112.06/103=1.1	-0.03	-0.27	48.60±3.00
15	3923	11:51:06.238	-28:46:49.59	1.86±0.37	2.18±0.42	16.90/20=0.85	-0.21	-0.05	43.60±8.40
16	4125	12:08:07.459	+65:10:28.59	2.02±0.10	3.95±0.24	127.16/123=1.03	-0.12	-0.21	79.00±4.80
17	4374	12:25:11.928	+12:51:53.67	2.11±0.09	6.35±0.34	139.83/136=1.02	-0.23	-0.15	127.0±6.80
18	4365	12:24:26.384	+07:16:53.04	0.94±0.22	1.66±0.23	30.97/33=0.94	0.43	-0.05	33.20±4.60
19	4473	12:29:42.631	+13:25:41.97	2.01±0.36	2.13±0.70	8.92/14=0.64	0	-0.29	42.60±14.00
20	4473	12:29:42.209	+13:25:10.73	1.76±0.42	2.55±0.45	11.09/14=0.80	-0.04	-0.09	51.00±9.00
21	4473	12:29:46.222	+13:24:32.11	1.51±0.37	3.15±0.71	10.15/14=0.73	0.14	-0.16	63.00±14.20
22	4473	12:29:58.294	+13:25:26.22	2.64±0.25	4.46±0.65	38.21/36=1.06	-0.25	-0.23	89.20±13.00
23	4473	12:29:50.319	+13:24:45.40	1.25±0.63	1.37±0.63	1.05/3=0.35	0.5	0	27.40±12.60
24	4494	12:31:29.590	+25:46:22.05	2.11±0.27	2.20±0.30	37.39/37=1.01	-0.18	-0.24	44.00±6.00
25	4494	12:31:28.569	+25:44:57.67	1.77±0.21	1.58±0.18	28.13/25=1.12	-0.07	-0.13	31.60±3.60
26	4649	12:43:45.005	+11:32:33.66	1.34±0.20	1.03±0.25	25.21/32=0.79	0.32	-0.28	20.60±5.00
27	4649	12:43:46.896	+11:32:34.15	1.26±0.14	2.38±0.22	72.46/70=1.03	0.16	-0.01	47.60±4.40
28	4697	12:48:46.858	-05:48:53.45	1.42±0.13	1.79±0.21	58.21/50=1.16	0.08	-0.24	35.80±4.20
29	4697	12:48:39.324	-05:48:07.20	1.44±0.19	1.13±0.17	23.63/28=0.85	0.04	-0.23	22.60±3.40
30	4697	12:48:33.225	-05:47:41.86	1.43±0.14	1.16±0.14	24.37/32=0.76	0.07	-0.18	23.20±2.80
31	5813	15:01:16.535	+01:41:34.19	2.06±0.10	7.37±0.39	113.97/139=0.82	0.03	-0.22	147.4±7.80
32	5813	15:01:10.859	+01:41:42.81	2.07±0.19	1.61±0.19	59.79/48=1.24	0.11	-0.26	32.20±3.80
33	5813	15:01:04.903	+01:41:36.16	1.56±0.25	3.36±0.44	40.42/54=0.75	0.42	0.12	67.20±8.80
34	5813	15:01:05.575	+01:43:30.80	1.96±0.25	1.94±0.22	41.00/49=0.84	0.26	-0.18	38.80±4.40

Note: Col.2 - galaxy name, Col.3 & 4 source position i.e. RA & DEC, Col.5 - power-law photon index Γ Col.6 - source luminosity, Col.7 - chi square per degree-of-freedom, Col.8 & 9 - hardness-ratio, where as SC=(M-S)/(H+M+S) and HC=(H-M)/(H+M+S). col.10 - black hole mass

the low-state objects to be lower than those of the high-state objects.

The low-state objects with lower L_X (compared to high-state) imply that, they may indeed be accreting at a lower rate than the high-state objects (Winter et al. 2006). If these sources are accreting at a rate similar to the Galactic low/hard-state BHs ($0.1L_{Edd}$; Done & Gierliński (2003)). We can estimate mass of the accreting source using the relation given in the (Winter et al. 2006),

$$\frac{M_{BH}}{M_\odot} = \frac{L_{bol}}{0.1L_{Edd}} \quad (1)$$

where, L_{Edd} is the Eddington luminosity for $1M_\odot$ (1.3×10^{38} erg s^{-1}). We apply a 'bolometric correction' of $\sim 2 \times L_X$ to account for the flux emitted outside this band. Then the equation for the black hole mass becomes (Zampieri & Roberts 2009)

$$\frac{M_{BH}}{M_\odot} \simeq 200 \left(\frac{L_X}{10^{40} erg\, s^{-1}} \right) \quad (2)$$

where L_X is the measured value of X-ray luminosity of the source in 0.3-10.0 keV band. We have quantified masses of the black hole sources responsible for observed X-ray luminosities of ULXs and are listed in column 10 of Table 2 and are found to lie in the range between $20.6M_\odot$ to $147.6M_\odot$. These estimates are found to be consistent with those reported by Patruno & Zampieri (2008) and Zampieri & Roberts (2009).

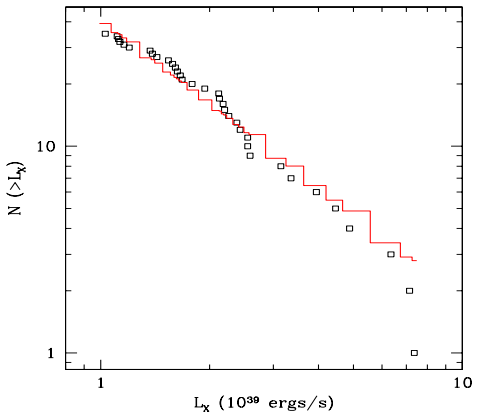

Fig. 4 The cumulative X-ray luminosity function (XLF) of all the 34 ULXs detected within sample of 15 galaxies, is well represented by a single power-law (solid red line)

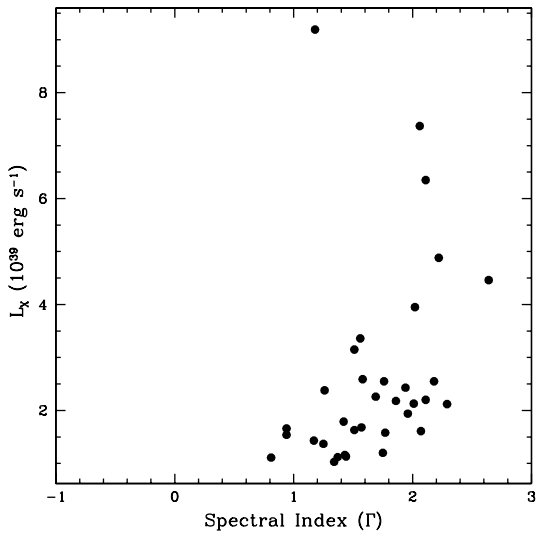

Fig. 5 The X-ray luminosity of ULXs plotted against their corresponding photon index value

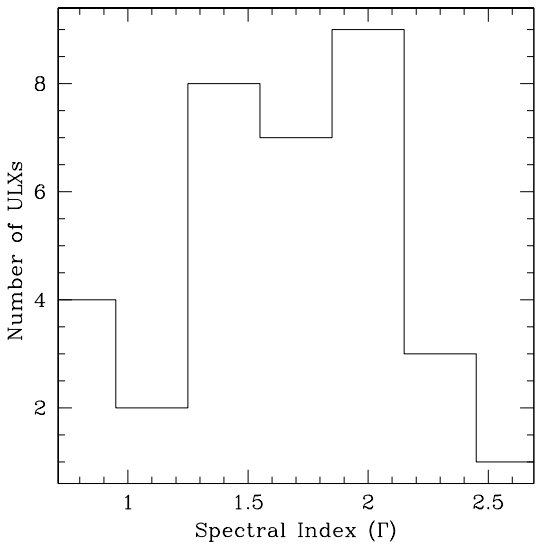

Fig. 6 Distribution of the spectral index Γ for low-state ULXs

Now it is clear that some of the X-ray sources in early-type galaxies are brighter than those seen in our Galaxy having isotropic emission above the Eddington limit of normal stellar mass BHs. It is debated what powers ULXs; models include (1) ordinary stellar mass BHs ($\leq 20M_{\odot}$), (2) massive stellar mass BHs ($20M_{\odot} \lesssim \mathbf{M} \lesssim 100\ M_{\odot}$) and (3) the intermediate mass BHs ($\mathbf{M} \sim$ 10^2 - $10^4\ M_{\odot}$).

(1) Stellar mass BHs: we do not find any source with mass $\lesssim 20M_{\odot}$ in the sample galaxies. These type of objects have been evidenced in the local universe (Feng & Kaaret 2009). In the Milky Way, the most massive stellar mass BH are those in GRS 1915+105 ($\mathbf{M}$ = 14.0 $\pm$4.4 $M_{\odot}$; Harlaftis & Greiner (2004)) and in Cygnus X-1 ($\mathbf{M}$ = 14.8$\pm$1.0 $M_{\odot}$; Orosz et al. (2011)). Remillard & McClintock (2006) found BHs in the Galaxy with mass in the range 3 $M_{\odot}< \mathbf{M} <$ 18 $M_{\odot}$.

(2) Massive stellar BHs: Among the 34 ULXs detected in present study, we find 31 as massive stellar mass BHs with mass in the range $20M_{\odot}$ to 100 $M_{\odot}$. Zampieri & Roberts (2009) have demonstrated an alternative scenario for the bright ULXs containing BHs with masses between $\sim$ $30M_{\odot}$ to $\sim$ $90M_{\odot}$, produced by stars with initial, main sequence mass above $\sim$ 40 - $50M_{\odot}$.

(3) Intermediate mass BHs: This type of sources ($\mathbf{M} \sim$ 10^2 - $10^4\ M_{\odot}$) are formed in young dense stellar clusters via runaway stellar merging,and have been successfully used to explain the most famous IMBH candidate ULX M82 X1 whose position is consistent with the star cluster MGG-11. In this scenario, the core collapse is driven by mass segrega-

tion in the dense cluster by core collapse of an isolated star (Ebisuzaki et al. (2001); Portegies Zwart et al. (2004)). In our sample we found three ULXs with luminosities $\gtrsim$ 4 - 8 $\times 10^{39}$ erg s^{-1}having mass in the range 100$M_{\odot}$to 150$M_{\odot}$.

5 Conclusions

In this paper we have presented detailed analysis of spectral properties of discrete X-ray sources having luminosity $>$ 10^{39} erg s^{-1} (ULXs) detected within D_{25} of 15 *Chandra* ACIS observations of the dusty early-type galaxies. Spectra of individual ULXs were fitted with an absorbed power law with photon indices between 0.81 to 2.64. Spectral fit parameters of 34 ULXs shows that these sources have high statistical probability of low (low/hard)-state sources. This study has revealed that majority of the ULXs in sample galaxies have massive stellar BHs having mass in the range between 20$M_{\odot}$ to 100 $M_{\odot}$. The comparison of the X-ray color-color plot for the ULXs exhibit a significant difference in the nature of the spectral indices of the sources. The combined XLF all the 34 ULXs is consistent with those reported earlier and is adequately described by a power-law with slope value -1.34$\pm$0.12.

6 Acknowledgments

This work is supported by UGC, New-Delhi under the major research project F.No. 36-240/2008 (SR-). We gratefully acknowledge the use of computing and library facilities of the Inter-University Center for Astronomy and Astrophysics (IUCAA), Pune, India. This work has made use of data from the Chandra data archive, NASAs Astrophysics Data System(ADS), NASA/IPAC Extragalactic Database (NED), provided by CXC.

References

Colbert, E. J. M. & Mushotzky, R. F., 1999, ApJ, 519, 89
Colbert, E. J. M. & Ptak, A. F., 2002, ApJS, 143, 25
Coleman Miller, M. & Colbert, E. J. M., 2004, International Journal of Modern Physics D, 13, 1
Dickey, J. M. & Lockman, F. J., 1990, ARA&A, 28, 215
Done, C. & Gierliński, M., 2003, MNRAS, 342, 1041
Ebisuzaki, T., Makino, J., Tsuru, T. G., et al., 2001, ApJ, 562, L19
Fabbiano, G., 1989, ARA&A, 27, 87
Fabbiano, G. & Trinchieri, G., 1987, ApJ, 315, 46
Feng, H. & Kaaret, P., 2009, ApJ, 696, 1712
Gilfanov, M., Grimm, H.-J., & Sunyaev, R., 2004, Nuclear Physics B Proceedings Supplements, 132, 369
Harlaftis, E. T. & Greiner, J., 2004, A&A, 414, L13
Irwin, J. A., Sarazin, C. L., & Bregman, J. N., 2002, ApJ, 570, 152
Kaaret, P., 2001, ApJ, 560, 715
Makishima, K., Kubota, A., Mizuno, T., et al., 2000, ApJ, 535, 632
Orosz, J. A., McClintock, J. E., Aufdenberg, J. P., Remillard, R. A., Reid, M. J., Narayan, R., & Gou, L., 2011, ApJ, 742, 84
Pandge, M. B., Vagshette, N. D., David, L. P., & Patil, M. K., 2012, MNRAS, 421, 808
Patruno, A. & Zampieri, L., 2008, MNRAS, 386, 543
Portegies Zwart, S. F., Dewi, J., & Maccarone, T., 2004, MNRAS, 355, 413
Prestwich, A., Zezas, A., Kaaret, P., Murray, S., Kilgard, R., Kim, D., & Schlegel, E., 2001, in IAU Symposium, Vol. 205, Galaxies and their Constituents at the Highest Angular Resolutions, R. T. Schilizzi, ed., pp. 208–+
Remillard, R. A. & McClintock, J. E., 2006, ARA&A, 44, 49
Roberts, T. P. & Colbert, E. J. M., 2003, MNRAS, 341, L49
Roberts, T. P. & Warwick, R. S., 2000, MNRAS, 315, 98
Sarazin, C. L., Irwin, J. A., & Bregman, J. N., 2000, ApJ, 544, L101
Soria, R., Risaliti, G., Elvis, M., Fabbiano, G., Bianchi, S., & Kuncic, Z., 2009, ApJ, 695, 1614
Strohmayer, T. E. & Mushotzky, R. F., 2003, ApJ, 586, L61
Swartz, D. A., Tennant, A. F., & Soria, R., 2009, ApJ, 703, 159
Vagshette, N. D., Pandge, M. B., Pandey, S. K., & Patil, M. K., 2012a, New A, 17, 524
Vagshette, N. D., Pandge, M. B., & Patil, M. K., 2012b, ArXiv e-prints
Winter, L. M., Mushotzky, R. F., & Reynolds, C. S., 2006, ApJ, 649, 730
Zampieri, L. & Roberts, T. P., 2009, MNRAS, 400, 677
Zezas, A., Fabbiano, G., Rots, A. H., & Murray, S. S., 2002, ApJS, 142, 239

This manuscript was prepared with the AAS LaTeX macros v5.2.